CONF-770802--2

PREPRINT UCRL-78892

Lawrence Livermore Laboratory

A Two-Phase Flow Cooling Concept for Fusion Reactor Blankets

D. J. Bender & M. A. Hoffman

January 14, 1977

This Paper was Prepared for Submital to the
1977 National Heat Transfer Conference
August 15-17, 1977
Salt Lake City, Utah

•

A Two-Phase Flow Cooling Concept for Fusion Reactor Blankets*

D. J. Bender

M. A. Hoffman

* Work performed under the auspices of the United States Energy Research & Development Administration Contract No. W-7405-Eng.-48

A Two-Phase-Flow Cooling Concept for Fusion Reactor Blankets

D. J. Bender and M. A. Hoffman

I. Introduction

The search for the "best" coolant for future fusion reactors employing magnetic confinement has been in progress for almost a decade now. However, the results of the conceptual design studies employing many different working fluids have been somewhat discouraging. Each of the coolants studied to date seems to have one or more serious drawbacks or difficulties associated with it. The principal coolants considered to date are derived mainly from fission reactor and space power supply technology; they include alkali metals (liquid lithium and boiling potassium), helium, molten salts such as flibe ($Li_2B_eF_4$) and water. The positive and negative characteristics of each of these coolants have been reviewed recently in References [1] and [2] in some detail. In addition, Reference [1] contains an impressive and sobering list of the many constraints and boundary conditions imposed by the magnetic fusion reactor environment which the thermal-hydraulics system designer must try to satisfy. We will only briefly summarize some of the principal findings to date and then discuss a new two-phase cooling conceot which has many of the desired characteristics for magnetic fusion reactors.

In order to obtain a tritium breeding ratio greater than unity the blanket surrounding the plasma must contain a large fraction of lithium (or lithium compound) and also must have a low structural fraction on the order of 5% to 10%. The low structure fraction minimizes the undesirable 14 MeV neutron-structure reactions, resulting in good neutron economy in the blanket. The thermal-hydraulic design is thus restricted to employing as low a coolant pressure as possible, since increasing coolant pressure requires increasing the amount of structure required to maintain the coolant pressure vessel (i.e., the blanket structure) integrity.

In order to have reasonably high thermal efficiency for the fusion powerplant, it is necessary to run the blanket at high peak temperatures somewhere in the range from 900 to 1100 K depending on the design goals. At the same time, it is highly desirable to have as uniform a temperature as possible throughout the blanket to minimize thermal stresses.

Liquid lithium is capable of operating at these high temperatures and requires only a relatively small temperature rise,typically less than 100°C,for energy absorption and transfer. However, the very large MHD pressure drop [2] occuring when this liquid metal traverses the high magnetic fields employed in these reactor designs results in very high coolant inlet pressures. This cooling scheme would thus require a high structural fraction in the blanket to take the large forces and possible excessive pumping power requirements as well.

Experience in the design of gas-cooled fission reactors has shown that helium pressured of about 50 atmospheres (5MPa) and He temperature rises of about 200 - 300 °C through the core are required to maintain an acceptably low pumping power. Helium thus violates the low pressure constraint. Nonetheless many conceptual design studies have been based on the use of helium coolant. The gas cooling schemes require relatively high coolant outlet temperatures from the blanket for high thermal efficiency. The use of a stainless steel structures limits the peak gas temperature to less than about 800 K, so that high temperatures can be obtained only by going to refractory metal alloys if the structural fraction is to be kept acceptably low. However, present indications are that at temperatures in excess of 900 - 1000 K, trace impurities in helium may cause severe corrosion problems in the refractory metals [1,3].

Water has been excluded as a possible working fluid at high temperature since the pressures would be intolerably high and corrosion problems would be unmanageable. These two considerations limit modern supercritical steam power plants to throttle steam conditions of about 1200 °F (~925 K) and 5000 psi (34 MPa) [4]. Also, water adds the complication of tritium contamination in the form of T_2O.

The flow of flibe in a magnetic field results in an MHD pressure drop which is much lower than that for the alkali metals, due to a significantly lower electrical conductivity. However, the V X B induced emf in the flibe (due to its finite electrical conductivity) may cause an unacceptable degree of decomposition of the flibe, and resultant corrosion of the structure [5] In addition, the strong magnetic fields tend to suppress the turbulence in the flow, resulting in very poor, near-laminar heat transfer coefficients for flibe. For these reasons flibe has been considered a poor coolant choice.

The use of boiling potassium has been proposed as a way to circumvent many of the above problems, and its many advantages are cited in Reference [1]. However, upon closer inspection, several problems with its use in magnetic fusion reactors have been identified. One of the most severe problems is related to magnetic effects. It was thought initially that the use of the enthalpy of vaporization of the potassium would result in low enough liquid flow rates at the inlets to the blanket modules to make the magnetic pressure drops negligible. However, a more detailed analysis has revealed that the pressures required to pump the liquid potassium across the magnetic field into the reactor blanket are high enough to cause serious stress problems in the inlet regions of conventional flow ducts [29].

In an attempt to take advantage of the many good features of boiling potassium, including its low-pressure, high-temperature capabilities, as well as the very low temperature gradients possible in the blanket structure, a new two-phase-flow concept is proposed in this paper which offers the promise of overcoming the above MHD problem.

2. Proposed Coolant Concept

The new two-phase heat transfer medium proposed is a mixture of potassium droplets and helium which permits blanket operation at high temperature and low pressure, while maintaining acceptable pumping power requirements, coolant ducting size, and blanket structure fractions.

For this particular study of a high-temperature, high-efficiency power plant, we assumed boiling potassium in the blanket at 900 - 950 °C to remove the blanket heat. The potassium vapor is then recondensed outside the blanket, rejecting the heat to a potassium topping cycle (which has an upper temperature of 850 °C). These conditions result in vapor pressures of 3 - 4 atm (0.3 - 0.4 MPa) in the blanket, and reasonable ducting sizes since the high vaporization enthalpy of potassium implies comparatively small mass flow rates. Th blanket cooling technique also has the advantage of a small fluid temperature change in the blanket (< 50 °C), resulting in a blanket structure with small temperature gradients and therefore relatively minor thermal stress problems. As has been demonstrated in the spacepower program, a number of structural materials such as Nb-1Zr are compatable with high temperature potassium [6,7].

However, transporting the liquid potassium into the blanket retains the problem of the MHD pressure drop. To circumvent this undesirable interaction, we have borrowed from experience gained in the development of two-phase liquid-metal MHD generators. Here, it was learned that in two-phase mixtures of liquid metal and a gas such as nitrogen or helium, the MHD interaction between the fluid and the B field essentially ceased for void fractions (ratio of helium volume to total fluid volume) in excess of about 85% [8,9]. This is due to the fact that at high void fraction, the flow can be in the form of liquid droplets dispersed in a continuous gas phase with the proper choice of gas flow rate and mixing scheme. In this state, the mixture exhibits the electrical conductivity of the gas phase, which is orders of magnitude lower than the liquid metal electrical conductivity. The ratio of liquid potassium density to helium density at 900 °C and 60 psia (0.4 MPa) is in excess of 3000, so that only a small He quality (He/total fluid mass fraction) is required. This fact, coupled with the low potassium flow rate mentioned above, results in low pumping power for the He flow as well as for the potassium flow.

A schematic of the primary heat transfer loop is shown in Figure 1. The two-phase flow is created in the mixer section, where the liquid potassium is injected into the helium flow, the potassium undergoing atomization and thus taking the form of small liquid droplets dispersed in the gas phase [10a]. The two-phase mixture is then transported into the blanket. We have assumed, in our analysis, that there is negligible MHD interaction in this mist flow regime.

As the two-phase mixture passes through the heat generating region in the blanket, the potassium droplets are vaporized. To obtain the high heat transfer coefficients typical of nucleate boiling in potassium, the boiler tubes in the blanket contain twisted helical inserts. [11,12] These inserts centrifuge the liquid droplets against the tube wall, where they undergo boiling and are vaporized. Thus the boiling process involves transferring heat from the tube wall directly to the liquid, resulting in a high heat transfer coefficient. Without the inserts, the heat would have to be transferred through the gas phase into the liquid droplets, resulting in a low heat transfer coefficient and therefore a considerable higher tube wall temperature and a larger heat transfer area. The penalty paid for employing the inserts is a higher pressure drop than would occur without the inserts, since the inserts increase the surface area and fluid velocity.

The boiler is designed to vaporize 80% of the potassium flow, i.e., the potassium exit quality from the fuel region is 0.8. Data on boiling with helical inserts [10,11] indicate that the inserts cannot sustain the high boiling heat transfer coefficients much above an 80% quality.

The flow leaving the blanket is thus a mixture of "wet" potassium vapor and helium which should experience no MHD forces. This flow is transported to a heat exchanger, where the potassium is recondensed, rejecting the blanket heat (plus pumping power) to the potassium topping cycle. The condensation of the potassium separates the potassium and helium flows, and the two fluids are drawn off separately from the heat exchanger. Also shown in Figure 1 is a separator, which may be required if there is some carry-over of potassium liquid in the He stream. The helium is compressed in a multistage compressor, the potassium pressure raised in a pump, and the two flows combined in the mixer before re-entry into the blanket.

We also note that the He/liquid metal two-phase flow technique is amenable to the design of a non-boiling blanket heat transfer loop, if the specific heat capacity of the sub-cooled liquid is used to remove the blanket heat. Thus, one could contemplate the use of a He/Li two-phase, mist flow working fluid, which performs both the heat removal and T_2 breeding functions in the blanket.

In summary, for the thermal-hydraulic calculations which follow, we have tried to select empirical equations for the friction and heat transfer coefficients keeping in mind the following desired flow conditions:

(1) Mist-annular two-phase flow regime in the initial low quality regions near the inlet which should make the magnetic field effects negligible.

(2) Nucleate boiling heat transfer regime in the submodule flow tubes due to the presence of helical inserts in these tubes.

Several key questions arise which bear upon the feasibility of this two-phase flow concept.

. Will the boiling hydrodynamics be influenced by the magnetic field?

. What mass fraction of helium is required?

. Will the flow separate due to centrifugal forces when the ducting changes direction, i.e., in bends, joints, etc?

At this time, there is not a sufficient data base on this particular type of flow to ascertain with sufficient confidence the feasibility of the proposed concept. However, in the following discussion we have used some general concepts and reasonable extrapolations of two-pnase flow data to determine representative characteristics of the potassium-helium mixture.

The effect of a magnetic field on the boiling hydrodynamics in potassium is unresolved. The one experimental study of which we have knowledge concluded that there were only very small effects due to the magnetic field.[13] However, this was a non-flowing pool-boiling experiment, quite different from the fusion reactor forced convective flow with which we are concerned.

In the following sections, we discuss the two-phase flows hydrodynamics and the details of the blanket thermal-hydraulic design. Brief descriptions of other components of the primary heat transfer loop and the thermal conversion system are then given and the overall power plant performance is summarized.

3. Two-Phase Flow Model

At this point, we focus on developing parameters for the two-phase inlet flow which will permit transport of the coolant into the blanket with a negligible MHD interaction.

3.1 Hydrodynamics of the Inlet Flow

The quality χ, and void fraction, α, of a two-phase flow are related by the equation [10b]

$$\frac{1-\chi}{\chi} = \frac{1}{k}\,\frac{\rho_{\ell}}{\rho_g}\,\frac{1-\alpha}{\alpha}, \qquad (1)$$

where ρ is density and k is the slip ratio (ratio of gas velocity to liquid velocity)

$$k = V_g/V_{\ell} \qquad (2)$$

In the following discussion, the subscript ℓ is used to denote potassium liquid and g denotes helium gas.

The conceptual blanket design, described in the subsequent section, has inlet flow conditions of approximately 360 °C and 60 psia (0.41 MPa), which result in the densities ρ_{ℓ} = [illegible] kg/m^3 and ρ_g = 0.171 kg/m^3 [14,15].

Equation (1) can then be rewritten as

$$X = \frac{k}{k + 3730\,\frac{(1-\alpha)}{\alpha}} \tag{3}$$

Thus the quantity of helium required for the flow is a function of the slip ratio, which is a complex function of many variables. Wallis [10a] indicates that the slip ratio is dependent on initial conditions (orifice design and flow characteristics in the mixer). In addition, downstream of the mixer the response of the droplets to the gas flow is dependent on the drop size [16], i.e., proportional to drag forces/inertia forces. However, in keeping with the preliminary nature of the present study we will evaluate a representative value of the slip ratio from existing two-phase flow correlations, realizing that the result will only be an approximation to the value which might be achieved in a flow loop designed to minimize interphase slip [8,9].

A two-phase flow regime map is shown in Figure 2. The coordinates in the figure are the gas and liquid velocity numbers which are expressed, respectively, as

$$NG = V_{sg}\left(\frac{\rho_g}{\sigma g}\right)^{1/4}, \tag{4}$$

$$NL = V_{s\ell}\left(\frac{\rho_\ell}{\sigma g}\right)^{1/4}. \tag{5}$$

Here, σ is surface tension, g is gravitational acceleration and V_s is the superficial velocity, defined as

$$V_{sg} = \frac{\dot{m}_g}{\rho_g A} = \alpha V_g \tag{6}$$

$$V_{sl} = \frac{\dot{m}_l}{\rho_l A} = (1-\alpha)V_l \tag{7}$$

where $\dot{m}$ is the flow rate and A is the duct cross-sectional area. Although the flow regime map is for horizontal flow, the authors [17] state that the boundaries of the liquid-phase-continuous and gas-phase-continuous regions are essentially independent of orientation. From the above relations, the slip ratio can be expressed as

$$k = \frac{NG}{NL}\,\frac{(1-\alpha)}{\alpha} \tag{8}$$

Our desired regime of operation, the gas-phase continuous, is characterized by $NG \gg NL$ while from the two-phase MHD results we require α on the order of 0.85 for negligible MHD interaction. Thus Equation (8) shows that this type of flow will exhibit slip ratios much larger then one.

The gas-phase-continuous regime is also known as "mist-annular" flow. Within this regime, at low values of NG (low superficial gas velocities) annular flow occurs with a liquid film on the wall and a central gas core. As the gas velocity increases, some of the liquid film is entrained in the gas core as droplets. Wallis [10a] has proposed the following correlation for the onset of entrainment

$$\frac{V_g \mu_g}{\sigma}\left(\frac{\rho_g}{\rho_l}\right)^{1/2} \geq 2.5 \times 10^{-4} \tag{9}$$

where μ is viscosity. This criterion for air-water flows at 1 atm and 70 °F implies NG ≳ 175 ± 100. This value of NG corresponds to the lower left-hand boundary in Figure 2 of the gas-phase-continuous regime for low NL. At higher values of NG, the fraction of the flow that is entrained is a function of NL, as shown qualitatively in Figure 3. It has been found that no matter how large NG, some of the liquid will always remain on the tube wall as a film, and this explains the low entrainment fractions for low NL. However, as NL is increase, the mass flow of liquid in the film remains about the same, and the increased flow occurs as droplets in the gas phase. For high enough NL, the mass flow in the wall film is small compared to the entrained mass flow and thus it can be assumed that essentially all of the liquid is entrained.

Due to the complex nature of entrainment flows, the entrainment fraction has not yet been successfully correlated. We thus select representative values of the flow parameters for the He/K mixture from air-water data, since the properties of the two mixtures are quite similar, as shown in Table 1.

HYDRODYNAMIC PROPERTY DATA

Table I

	Air-water 1 atm., 20 °C	He/K[14,15] 4 atm., 900 °C
ρ_ℓ (kg/m^3)	1000	638
ρ_g (kg/m^3)	1.15	.171
μ_ℓ (N-s/m^2)	9.8×10^{-4}	1.4×10^{-4}
μ_g (N-s/m^2)	1.8×10^{-5}	5.0×10^{-5}
σ (N/m)	7.2×10^{-4}	5.7×10^{-4}

For the flow under consideration, complete entrainment of potassium in He is the desired operating mode and we select the following parameters based on air-water data [18,19],

$$NG = 500 \ ,$$

$$NL = 5 \ .$$

[illegible]sing the property data in Table I, these values of the velocity numbers yield V_{sg} [illegible] m/s and V_{sl} [illegible] m/s.

[illegible]ubstitution of Equation (8) into (2) gives an expression for the [illegible]uality as a function of the velocity numbers,

$$[illegible] \left(1 + [illegible] \frac{N_L}{N_G} \right)^{-1} \ , \qquad (10)$$

which then evaluates to

$$[illegible]$$

[illegible] calculate the void fraction, we select the Dartmouth correlation [10d] because of the extensive data base which it represents,

$$\frac{V^*_{sg}}{1+3.1\,[illegible](1-\alpha)} + \frac{V^*_{sl}}{3.1(1-\alpha)} = 1 \ , \qquad (11)$$

where

$$V^*_{sg} = V_{sg} \left(\frac{[illegible]}{gD} \right)^{1/2} \ , \qquad (12)$$

$$V^*_{sl} = V_{sl} \left(\frac{[illegible]}{gD} \right)^{1/2} \ . \qquad (13)$$

and D is the duct diameter. However, Equation (11) must be used with caution since it is based on data from air-water flows with a maximum of 20% entrainment, $V_{sg}^* < 2.5$, $V_{s\ell}^* < 1$, and $D = 2.5$ cm. Equation (11) may be rewritten as:

$$\frac{NG\sqrt{\rho_g/\rho_\ell}}{1-3.1(1-\alpha)} \qquad \frac{NL}{3.1(1-\alpha)} = \left(D\sqrt{\frac{\rho_\ell g}{\sigma}}\right)^{1/2} . \qquad (14)$$

From details of the blanket design described in the subsequent section, we determined D = 0.4 m and thus Equation (14) yields

$$\alpha = 0.81 ,$$

and from Equation (8)

$$k = 23,$$

and $V_{sg}^* = 0.71$, $V_{s\ell}^* = 0.43$. This value of the void fraction is approximately the same as the value in the two-phase liquid metal MHD flows that resulted in a decoupling between the flow and the B field ($\alpha \gtrsim 0.85$), and thus provides support for the flow parameters and correlations we have chosen to model the flow. As a basis of comparison, correlations from other investigators for the void fraction were evaluated for our flow parameters and these results are presented in Table 2.

A Comparison of the Evaluation of

Various Void Fraction Correlations

Table 2

Ref	α	k
[10d] our eq. (14)	0.81	23
[25], [10f]	0.78	25
[26]	0.75	15
[10e]	0.85	18

The agreement between the various correlations can be seen to be quite good for both α and k, considering the restricted nature of most of the correlations.

The key objective in this new two-phase flow concept is to eliminate the MHD pressure drop at the inlet. The data of References 8 and 9 indicate that for our estimated value of $\alpha \gtrsim .81$, we are very close to accomplishing this objective (i.e. the electrical conductivity should be negligible). Other data on two-phase NaK/N_2 flows in a magnetic field [27,28] seem to indicate that a somewhat higher α may be required. For the experiments of Refs. [27,28], flow parameters were $NG \gtrsim 400$-600 and $NL \simeq 5$-10. It was found that (1) the mixture electrical conductivity was reduced by a factor of 200 - 300 below that of pure NaK for $\alpha \gtrsim 0.95$, and (2) the pressure drop was a factor of 2 - 3 greater, at B=0.8 Tesla, than with B=0. Comparing these results to the present flow design, we note that the velocity numbers in the experiment are similar to those chosen for the blanket design. A significant reduction in the liquid metal conductivity did occur in the experiments, although there was still some residual MHD interaction. Thus we conclude that our concept is conceptually correct, but

Due to the preliminary nature of our model some refinement may be required in the choice of velocity numbers to reduce the MHD pressure drop to a negligible level.

We now address the question of the two-phase flow behavior in the pipe bends. Here, the flow regime map of Farukhi and Parker [20] is used (see Figure 4). The coordinates are dimensional with English Engineering Units being used except for [illegible]. Evaluating the flow quantities based on the parameters calculated above, we obtain

$$G_g/\lambda = 1.6 \times 10^4 ,$$
$$G_l\psi = 4.75 \times 10^2 ,$$

which appears as the point • in Figure 4. The flow map indicates that mist-annular flow should be sustained in the piping bends, but experimental verification of this for the particular bend radii of a specific design is felt to be necessary.

3.2 Helium Pumping Power

Another consideration, which relates to the economic feasibility of this two-phase concept, is the pumping power requirement for the helium. To assess the helium pumping power, we have assumed the use of two compressors with an intercooler. A process diagram for the He compression is shown in Figure 5. The numbers on the diagram correspond to the station numbers shown in Figure 1.

The compression process from "g" to "a" (low compressor) is described by

$$\frac{T_a}{T_g} = 1 + \left(\frac{1}{\eta_c}\right)\left[\left(\frac{p_a}{p_g}\right)^{\frac{\gamma-1}{\gamma}} - 1\right] \qquad (15)$$

where γ is the specific heat ratio and η_c is the compressor isentropic efficiency. A similar equation describes the high compressor from "b" to "2". The inter-cooling process is characterized by an intercooler effectiveness,

$$\varepsilon_g = \frac{T_a - T_b}{T_a - T_g} . \qquad (16)$$

The compressor input power is:

$$\dot{W}_{HG} = \dot{m}_g c_p \left[(T_a - T_g) + (T_2 - T_b)\right] . \qquad (17)$$

Now assuming equal pressure ratios, $p_a/p_g = p_2/p_b$ (which minimizes $\dot{W}_{HG}$), and defining a compression ratio

$$r_p = \frac{p_2}{p_g} ,$$

Equations (15 and 16) can be substituted into (17) to yield

$$\dot{W}_{HG} = \dot{m}_g c_p \, T_g \, [\text{illegible}] \left[[\text{illegible}] \right] .$$

where F_p is defined as

$$F_p = \left(\frac{1}{\eta_c}\right)\left[(r_p)^{\frac{\gamma-1}{\gamma}} - 1\right] \quad . \tag{19}$$

To place the pumping power in perspective, it is a typical procedure to normalize it to the blanket thermal power,

$$\dot{q}_{BL} \approx \dot{m}_K \, \Delta h_K \ ,$$

where Δh_K is the potassium boiling enthalpy rise in the blanket; the He contribution is negligible. Thus,

$$\frac{\dot{W}_{He}}{\dot{q}_{BL}} = \frac{x}{1-x} \, \frac{c_p T_g}{\Delta h_K} \, F_p \left[2 + F_p(1-\epsilon_N)\right] \quad . \tag{20}$$

To evaluate Equation (20), we take component performance figures from Reference 21, $\eta_c = 0.89$, $\eta_N = 0.98$. For the helium $\gamma = 5/3$, $c_p = 5165$ J/kg°K and $T_g =$ 1173 K (900 °C). For potassium, $\Delta h_k = 1.53 \times 10^6$ J/kg (658 Btu/lbm) for an 80% exit quality from the blanket at 900 °C. The pumping to thermal power ratio is plotted in Figure 6 as a function of He quality and pressure ratio.

Typically, gas-cooled fission reactors have a pumping to thermal power ratio of 3 - 4 %. If we restrict the operation of our blanket flow loop to this range of values, the He pressure ratio must be less than about 2.

An interesting modification to the cycle is the possibility of injecting some saturated-liquid potassium droplets into the He inlet flow to the compressor. Some of the compressor power is absorbed by the liquid potassium, resulting in a smaller temperature rise and thus a reduced pumping power.

[illegible] have been tested [illegible] the [illegible] conditioning system. The presence of [illegible] the [illegible] would not alter the operation of the heat transfer [illegible] is mixed with He just downstream of the [illegible]. However, the potassium droplets in the He flow might [illegible], alter the [illegible] design and maintenance requirements.

4. Primary Heat Transfer Loop

Here, we describe the blanket design and the thermal hydraulic analysis of the primary heat transfer loop, which incorporates the two-phase flow concept.

4.1 Blanket Description

The analysis described in this paper was part of the conceptual design of a mirror fusion reactor. The reactor uses a Yin-Yang coil to provide plasma confinement in a magnetic well. The blanket has the shape of a spherical shell that resides inside the magnet coils as shown in Figure 2. The blanket is divided vertically into 16 [illegible] segments, or modules, each with its own coolant ducting.

The plasma produces 1270 MW of fusion power giving a first wall neutron loading of 3.5 MW/m^2, and a blanket energy multiplication of 1.69 yields 1720 MW of thermal power in the blanket. The blanket power is used to produce potassium vapor at 850 °C on the secondary side of the heat exchanger (shown in Figure 1), the 850 °C vapor being used in the turbines of a potassium topping cycle.

A cross-section through a blanket module is shown in Figure 8. The two-phase flow is transported into the blanket in a common inlet plenum, distributed to the submodules where the potassium is vaporized (to 80% quality) and then collected from the submodules and transported out of the blanket. The blanket "fuel", contained in cans in the submodules, is a mixture of beryllium and lithium beryllate (Li_3BeO_4) to provide energy multiplication and tritium breeding. The fuel cans are designed with axial coolant passages which contain helical inserts as shown in Figure 8.

The thermodynamic conditions around the loop are summarized in Table 4 (based on calculations to be described in the next sections), and were determined based on the constraints of the 850 °C vapor in the potassium topping cycle and a maximum blanket fuel temperature of 1000 °C. The total blanket requires a flow of 4.2 X 10^6 kg/hr of potassium and 1.1 X 10^5 kg/hr of helium, using the He quality of 0.026 determined previously. The helium compressor, operating through a pressure ratio of 1.31, has an input power requirement of 27 MW, or 1.6% of the blanket thermal power.

Thermodynamic State Variables for the Blanket Thermal Transport Loop

Table 4

	POTASSIUM				HELIUM	
Station #	p (psia) (MPa)	T °F (°C)	h Btu/lbm (MJ/kg)	Quality	p (psia) (MPa)	T °F (°C)
1	[illegible]	[illegible]	[illegible]	[illegible]**		
2					[illegible]	[illegible]
3	[illegible] (.40)	1696 (924)	[illegible]	[illegible]	[illegible]	[illegible]
4	[illegible]	[illegible]	[illegible]		[illegible]	[illegible]
5	[illegible]	[illegible]	[illegible]	[illegible]	[illegible]	[illegible]
6	[illegible]	[illegible]	[illegible]	[illegible]	[illegible]	[illegible]
7	[illegible]	[illegible]	[illegible]	[illegible]*	[illegible]	[illegible]
8	[illegible]	[illegible]	[illegible]	[illegible]		
9					44	[illegible]

* [illegible]

** [illegible]

4.2 Blanket Thermal Design

The design of the submodule fuel can and the unit cell used for the thermal analysis are shown in Figure 9. For this analysis the presence of the He was neglected since the temperature change in the blanket and the He mass fraction (2.6%) are small.

The neutron-induced heat generation profile can be approximated by an exponential,

$$\dot{q}''' = \dot{q}_0''' \, e^{-\lambda z}, \tag{21}$$

where $\dot{q}_0'''$ is the fuel power density at the front of the fuel region (first wall) and z is the axial coordinate along the coolant tube outward through the fuel region. For our blanket design, $\dot{q}_0''' = 23$ w/cm^3, [illegible] = 3.06 m^{-1} and the length of the fuel region is $L = 0.8$ m.

The initial variables to be determined in the thermal analysis are the coolant tube diameter, d_t, and coolant tube pitch, P_t. The constraints on the design are (1) the fuel temperature must not exceed 1000 °C, (2) the heat flux must not exceed the critical heat flux, and (3) the pressure drop must be small enough to result in a pressure ratio across the compressor [illegible].

The tube diameter and pitch were determined by applying a heat balance and the thermal conduction equation to the unit cell shown in Figure 9. The thermal conductivity of the sintered Be fuel was assumed to be 1/2 of that for the pure metal (to account for voids) and a potassium mass flux of G_K = [illegible] lbm/hr-ft^2) was used which is typical of the values used in the boiling potassium tests with helical inserts [11,12]. The boiling heat transfer coefficient was calculated from the correlation [12]

$$h_B = .0016\,(p/d)_h\,(1 + a_R)^{0.16}\,(\hat{q}''_w)^{1.16}\ \mathrm{Btu/hr\text{-}ft^2\text{-}°F}. \qquad (22)$$

Here, $(p/d)_h$ is the helix pitch-to-diameter ratio, and $\hat{q}''_w$ is the wall heat flux ($\mathrm{Btu/hr\text{-}ft^2}$). The symbol a_R denotes the radial acceleration of the flow induced by the helical insert,

$$a_R = \frac{2}{g d_t}\left[\frac{\pi}{(p/d)_h}\,\frac{(1 - X_K)}{(1 - \alpha)}\,\frac{G_K}{\rho_f}\right]^2, \qquad (23)$$

which is expressed in g's (i.e., multiples of the gravitational acceleration). In the absence of any data, the effect of the magnetic field on the wall film (created by the inserts centrifuging the liquid drops against the wall) was neglected. A potassium exit quality of 80% was used, as the correlation Equation (22), is only valid below this quality. For higher quality, there is not enough liquid in the flow to maintain a continuous film on the wall and the heat transfer coefficient decreases significantly.

The analysis resulted in the dimensions

$$d_t = 0.70\ \mathrm{cm},$$
$$\ell_t = 3.90\ \mathrm{cm},$$

with $(p/d)_h = 9$ and a total heat transfer area for the blanket of about 3800 m^2. The peak fuel temperature occurs at the inlet ($z = o$), and the radial temperature profile is plotted for this position in Figure 10. The fuel center temperature of 1013 °C was judged sufficiently close to the specified value of 1000 °C, given the uncertainties in the fuel conductivity and boiling heat transfer coefficient.

The critical value of the heat flux is that value where a vapor film forms on the wall and the heat transfer coefficient drops drastically below that for nucleate boiling (often resulting in "burn-out"). The critical heat flux for boiling potassium with helical inserts is given by the correlation [11],

$$\dot{q}''_c = \frac{(1 + a_R)^{1/4} \times 10^6}{1 + \left(\frac{2X_k}{1 - X_k}\right)} \quad \text{Btu/hr-ft}^2 \qquad (24)$$

where x_K is the potassium quality. For the present design, $\dot{q}''_w / \dot{q}''_c \simeq 0.4$ at the inlet ($\dot{q}''_w \simeq 125$ w/cm^2) and this ratio decreased monotonically to the exit where it had the value of about 0.07. The design heat flux was judged to be sufficiently below the burn-out value.

In our present design, we have used the twisted inserts in the fuel coolant tubes. However, this design choice is not essential to the use of the two-phase (He/K) coolant concept. Without the inserts, a heat transfer coefficient lower than that given by Equation (22) would result as the heat transfer would occur through the gas component of the flow. Thus without the inserts d_t and δ_t would have to be re-evaluated to give a lower heat flux and thus a larger volume fraction of coolant and structure in the blanket.

4.3 Pressure Drop in the Primary Loop

Around the primary heat transfer loop, three different types of flows occur. First, the two-phase He/K liquid flow from the mixer to the fuel coolant tube inlet in the blanket; second, the boiling with inserts in the fuel coolant tubes; and third, the He - 80% potassium quality flow from the fuel coolant tube outlet to the heat exchanger.

The inlet He - K liquid flow pressure drop was evaluated from the data of Reference 23, where it was found that for high-NG, high-entrainment, flows the pressure drop is approximately twice the pressure drop that would be calculated if the liquid were not present. This relation is shown in Figure 11. The effective two-phase dynamic head is thus

$$P_d = 2\left(\frac{\rho_g V_{sg}^2}{2}\right) \quad . \tag{25}$$

Using NG = 500, we obtain a dynamic head of 0.18 psi (1.24 kPa) and a pressure drop for this inlet flow of 1.2 psi (8.3 kPa). From the values of NG, NL and the mass flow rates, all the inlet ducting sizes can be evaluated. The required inlet flow area is only 0.13 m^2 per module (1/16 of total flow), the inlet duct diameter is 0.4 m and the inlet plenum width (see Figure 8) is t_{PL1} = 0.03 m.

The boiling pressure drop in the fuel has two components, one due to acceleration and one due to friction. In the calculation of the pressure drop, the He must be included since the He volume flow rate is equal to approximately 30% of the potassium vapor volume flow rate exiting from the fuel region.

The acceleration pressure drop is simply the difference in dynamic head between inlet and outlet. To treat all three components of the flow (He, K liquid, K vapor), the homogenious model [24] was used to define an average fluid density and resulted in an acceleration pressure drop of 1.2 psi (8.3 kPa).

The frictional pressure drop was calculated with the homogeneous model [24], using a density based on an average potassium quality (through the length of the tube) of $\chi_k = 0.39$. The resulting average density was used in the frictional pressure drop model for adiabatic flow in a tube with a helical insert. [11] These assumptions yielded a frictional pressure drop of 6.1 psi (42.1 kPa), and thus a pressure drop in the fuel of 7.3 psi (50.3 kPa). As can be seen in Table 4, the potassium temperature shows the unusual feature of decreasing through the blanket. This is due to the fact that the inlet flow is an almost saturated liquid and the flow undergoes a pressure drop through the blanket during heat addition. This process is illustrated in Figure 12.

The space available for outlet ducting from the blanket dictated a dynamic head of 0.85 psi (5.86 kPa), which was evaluated using the Martinelli two-phase adiabatic flow model [24], and accounted for all three components of the flow. The resulting outlet plenum flow passage height was $t_{PLO} = 0.12$ m (see Figure 8). The outlet duct diameter, using the co-axial scheme shown in Figure 8, was 1.12 m. The pressure drop for this portion of the flow, from fuel outlet to heat exchanger inlet, was estimated to be 3.0 psi (20.7 kPa). The resulting pressures at various points in the cycle are summarized in Table 4.

Although we were admittedly optimistic about the number of head losses in the inlet/outlet ducting, the modest 1.6% ratio of He pumping power to blanket thermal power implied that the inlet/outlet ducting pressure drop (which is 30% of the total) could be significantly larger than estimated without incurring excessive pumping power requirements.

5. Conclusions

A new two-phase flow concept for magnetically confined fusion reactors has been proposed to overcome the MHD pressure drops at the inlet of a boiling potassium cooling system. Preliminary calculations indicate that the addition of about 2.6% of helium mass flow to the liquid potassium inlet flow can create an annular-mist flow where the magnetic field effects are negligible. Furthermore the overall loop pressure drop for the helium is about 23% resulting in a ratio of helium pumping power to thermal power of only 1.6%. While we can conclude that the concept looks promising on the basis of this preliminary study, several aspects of the thermal-hydraulic correlations used require experimental verification.

REFERENCES

1. A. P. Fraas, "Comparative Study of the More Promising Combinations of Blanket Materials, Power Conversion Systems, and Tritium Recovery and Containment Systems for Fusion Reactors", Oak Ridge National Laboratory Report ORNL-TM-4999, November 1975.

2. M. A. Hoffman, R. W. Werner, G. A. Carlson and D. N. Cornish, "A Review of Heat Transfer Problems Associated With Magnetically-Confined Fusion Reactor Concepts", Lawrence Livermore Laboratory Report UCRL-78036, April 1976.

3. L. A. Charlot and R. E. Westerman, "Helium Coolant Compatability With candidate Fusion Reactor Structural Materials", Pacific Northwest Laboratories Report BNWL-1842, July 1974.

4. J. H. Harlow, "Engineering the Eddystone Plant for 5000-lb 1200-Deg Steam", Trans. ASME, 79, p. 1410, 1957.

5. M. R. Grimes and S. Cantor, "Molten Salts as Blanket Fluids in Controlled Fusion Reactors", in The Chemistry of Fusion Technology, Gruen, D. M. (ed.), Plenum Press, N. Y. 1972 pp. 161-190.

6. S. V. Manson, "A Review of the Alkali Metal Rankine Technology Program", J. Spacecraft and Rockets, 5, 1249, November 1966.

7. T. A. Moss, "Materials Technology Presently Available for Advance Rankine Systems", Nuc. Applications, 3, 71, February 1967.

8. M. Petrick, "MHD Generators Operating with Two-Phase Liquid Metal Flows", in Electricity From MHD, Proc. of Intl' Symposium on MHD Power Generation, Salzburg, July 1966, p. 889.

9. W. E. Amend, M. Petrick and J. C. Cutting, "Analysis of Liquid-Metal MHD Power Cycles for Central Station Power Generation", Proc. of 12th Symposium on Engineering Aspects of MHD, Argonne Nat'l Laboratory 1972, p. IV.1.1

10. G. B. Wallis, One-Dimensional Two-Phase Flow, McGraw-Hill, 1969. /a/ Chap. 12, /b/ p. 13, /c/ p. 51, /d/ p. 353, /e/ p. 51, Eq. (3.32),/f/ p. 85, Eq. (3.122), /g/ p. 392.

11. J. R. Peterson, "High Performance 'Once-Through' Boiling of Potassium in Single Tubes at Saturation Temperatures of 1500° to 1750°F", General Electric Co., NASA Contractor Report no. NASA CR-842, August 1967.

12. J. A. Bond and G. L. Converse, "Vaporization of High Temperature Potassium in Forced Convection at Saturation Temperatures of 1800° to 2100°F", General Electric Co., NASA Contractor Report no. NASA CR-843, July 1967.

13. A. P. Fraas, D. B. Lloyd and R. E. MacPherson, "Effects of a Strong Magnetic Field on Boiling of Potassium", Oak Ridge National Laboratory Report ORNL-TM-4218, February 1974.

14. W. D. Weatherford, Jr., J. C. Tyler and P. M. Ku, "Properties of Inorganic Energy - Conversion and Heat-Transfer Fluids for Space Applications", Southwest Research Inst., WADD Technical Report 61 - 96, November 1961.

15. H. W. Hoffman and B. Cox, "A Preliminary Collation of the Thermodynamic and Transport Properties of Potassium", Oak Ridge National Laboratory Report ORNL-TM-2126, July 1968.

16. C. T. Crowe, "Vapor-Droplet Flow Equations", Lawrence Livermore Laboratory Report UCRL-51877, August 1975.

17. T. L. Gould, M. R. Tek and D. L. Katz, "Two-phase Flow Through Vertical, Inclined or Curved Pipe", J. Petroleum Technology, August 1974, p. 915.

18. M. Wicks, III, and A. E. Dukler, "Entrainment and Pressure Drop in Concurrent Gas-Liquid Flow: I. Air-Water in Horizontal Flow", AIChE J., 6, #3, 463 September 1960.

19. J. G. Collier and G. F. Hewitt, "Data on the Vertical Flow of Air-Water Mixtures in the Annular and Dispersed Flow Regions. Part II: Film Thickness and Entrainment Data and Analysis of Pressure Drop Measurements", Trans. Inst. Chem. Engrs., 39, 127 (1961).

20. N. M. Farukhi and J. D. Parker, "A Visual Study of Air-Water Mixtures Flowing Inside Serpentine Tubes", Heat Transfer 1974, Vol. IV, Proc. 5th Int'l Heat Transfer Conf., Tokyo, 1974, p. 205.

21. S. C. Kuo, "Closed-Cycle Helium Gas Turbines for UWMAK-III Fusion Power Generation", Final Report, United Technology Research Ctr., UTRC Report R75-952094-2, November 1975.

22. L. F. Lindsey, "ROVAC" How It Can Heat and Cool Your House, Popular Science, 209 #2, p. 84, August 1976.

23. K. Aziz and G. W. Govier, "Horizontal Annular-Mist Flow of Natural Gas-Water Mixtures", Can. J. Chem. Engr., 40, 51 (1962).

24. P. Griffith, "Two-phase Flow", in Handbook of Heat Transfer, Rohsenow and Hartnett (eds.), McGraw-Hill, Chapter 14.

25. Madsen, N., "A Void Fraction Correlation for Vertical and Horizontal Bulk Boiling of Water", Heat Transfer 1974, Vol. IV., Proc. 5th Int'l Heat Transfer Conf., Tokyo, 1974, p. 185.

26. Levy, S., "Steam Slip-Theoretical Prediction from Momentum Model", J. Heat Transfer, May 1960, p. 113.

27. G. H. Gelb, K. A. Sense, S. M. Zivi and L. G. Neal, "Electrical Conductivity of High-Void-Fraction Two-Phase Flow in an MHD Generator: I. Experiment", AIAA J., 5, #11, p. 2094 (1967).

28. K. A. Sense, "Electrical Conductivity of High-Void-Fraction Two-Phase Flow in an MHD Generator: II. Analysis", AIAA J., 5, #11, p. 2097 (1967).

29. Wells, W., Oak Ridge Nat'l Laboratory, Private Communication, 1976.

NOMENCLATURE

A	=	cross sectional area of duct
a_R	=	radial fluid acceleration due to twisted insert
c_p	=	He specific heat
D	=	duct diameter
d_t	=	coolant tube diameter in the blanket
f	=	Fanning friction factor, $f = \tau_w/(\rho v^2/2)$
G	=	mass flux
g	=	gravitational acceleration
h_B	=	boiling heat transfer coefficient
k	=	velocity slip ratio
$\dot{m}$	=	mass flow rate
NG	=	gas velocity number
NL	=	liquid velocity number
p	=	pressure
p_d	=	dynamic head
$(p/d)_h$	=	helical insert pitch-to-diameter ratio
$\dot{q}_{BL}$	=	blanket thermal power
$\dot{q}''_w$	=	heat flux in blanket coolant tubes
$\dot{q}''_c$	=	critical heat flux in the blanket coolant tubes
$\hat{q}'''$	=	blanket fuel power density
r_p	=	total pressure ratio across helium compressor
T	=	temperature
V	=	fluid velocity
V_s	=	fluid superficial velocity
$\hat{W}_{HE}$	-	helium compressor inlet power

α = void fraction

γ = He specific heat ratio

δ_t = coolant tube pitch in the blanket

ε_H = intercooler effectiveness for He compressor

η_c = He compressor isentropic efficiency

Λ = flow parameter, see Figure 4

μ = viscosity

ρ = density

σ = surface tension

χ = He quality (ratio of He/total mass flow)

χ_K = potassium quality (fraction of potassium mass flow in the vapor state)

Ψ = flow parameter, see Figure 4

Subscripts

g = gas (He)

ℓ = liquid (potassium)

K = potassium

n = (n=integer) station number defined in Figure 1

sg = superficial gas

sℓ = superficial liquid

PRIMARY HEAT TRANSFER LOOP SCHEMATIC

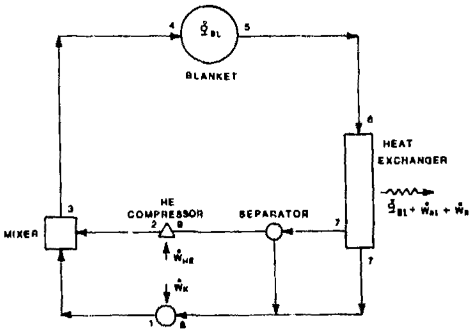

LOOP ARRANGEMENT

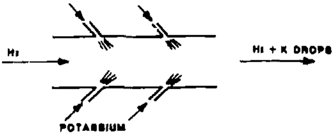

MIXER DETAIL

Figure 1

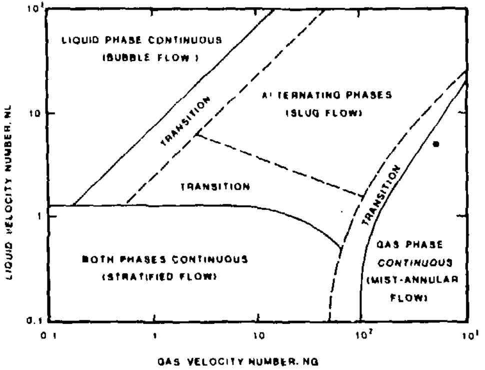

FLOW REGIME MAP FOR HORIZONTAL TWO PHASE FLOW.

BASED ON AIR WATER DATA (REF. 17)

● -DESIGN POINT

Figure 2

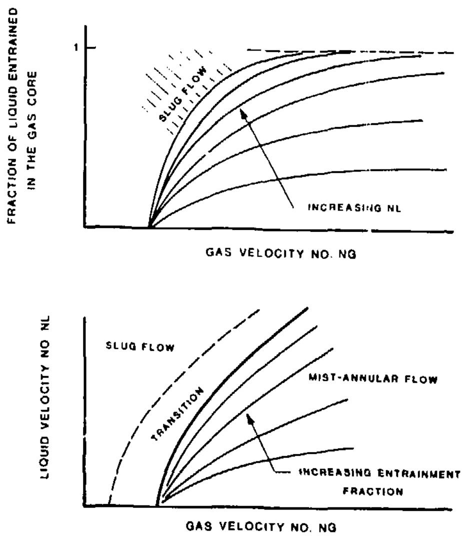

ENTRAINMENT CHARACTERISTICS IN
MIST-ANNULAR FLOW (REF. 10G)

Figure 3

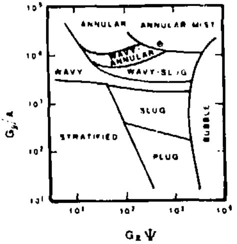

FLOW REGIME MAP FOR
HORIZONTAL SERPENTINE TUBES (REF 20)
●-DESIGN POINT

$G_L = \rho_L v_L (1-\alpha)$ LBM HR FT^2

$G_g = \rho_g v_g \alpha$ LBM HR FT^2

$\Lambda = \sqrt{\rho_L \rho_g}$ LBM FT^3

$\Psi = \mu_L^{1/3} / \sigma \rho_L^{2/3}$ CM FT$^{2/3}$/DYNES HR$^{1/3}$ LBM$^{1/3}$

Figure 8

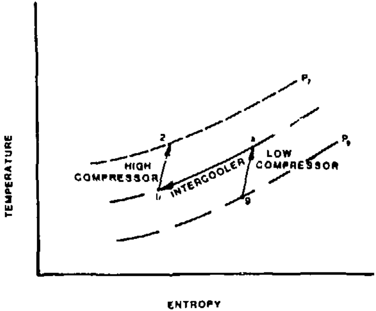

PROCESS DIAGRAM FOR HELIUM COMPRESSION

Figure 5

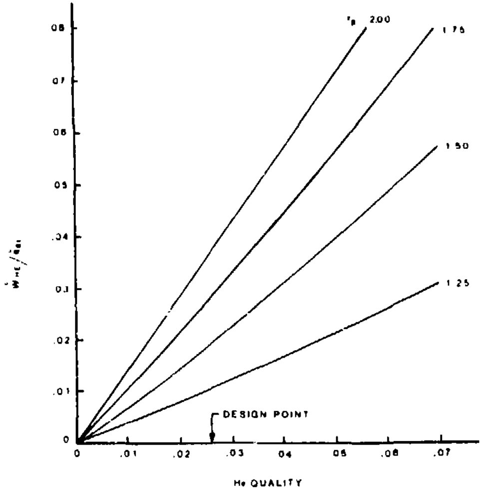

HELIUM PUMPING POWER NORMALIZED
TO BLANKET THERMAL POWER

Figure 6

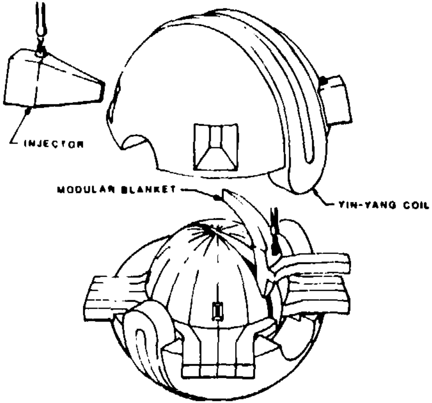

MIRROR REACTOR WITH SPHERICAL BLANKET

Figure 7

BLANKET FLOW GEOMETRY

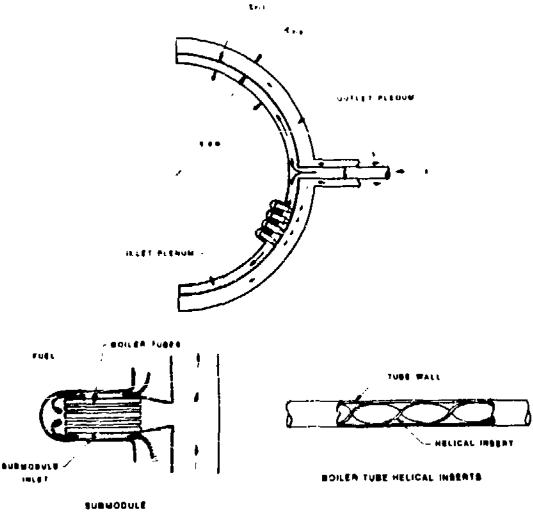

Figure 8

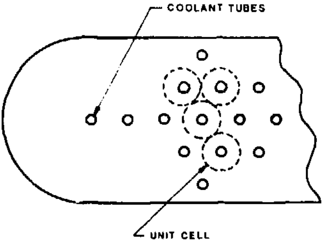

END VIEW OF FUEL CAN

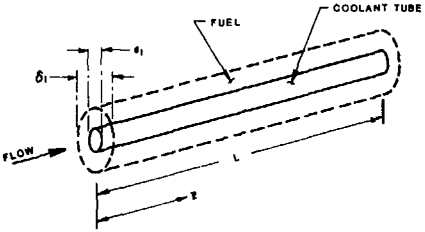

UNIT CELL DETAIL

Figure 9

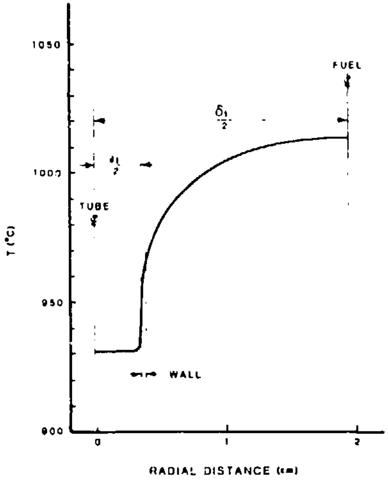

RADIAL TEMPERATURE PROFILE AT
FUEL REGION INLET

Figure 1

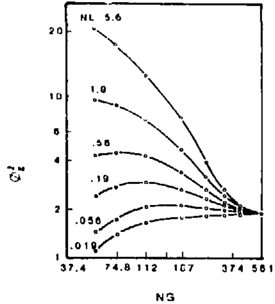

$$\frac{dp}{dl} = \phi_g^2 \left(4\frac{f}{d}\right)\left(\frac{\rho_g V_{sg}^2}{2}\right)$$

PRESSURE DROP IN TWO-PHASE
MIST-ANNULAR FLOW.
ADAPTED FROM REF. 24.

Figure 11

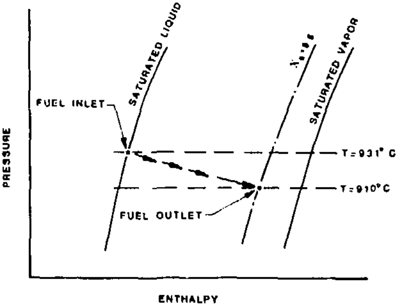

THERMODYNAMIC REPRESENTATION OF THE
BOILING PROCESS IN THE BLANKET FUEL

Figure 12